Eur. J. Mineral.
2003, **15**, 641–647

Experimental evidence on phlogopitic mantle metasomatism induced by phengite dehydration

BERND WUNDER[1]* and STEFAN MELZER[2]

[1] GeoForschungsZentrum Potsdam, Department 4, Telegrafenberg, D-14473 Potsdam, Germany
* Corresponding author, e-mail: wunder@gfz-potsdam.de
[2] Ceramics Research Centre, Corus RD&T, NL-1970 CA Ijmuiden, The Netherlands

Abstract: To simulate metasomatism at convergent plate boundaries, the process of phengite dehydration, followed by reactions between the expelled fluid and a model mantle material consisting of forsterite + enstatite, was investigated at subduction zone conditions using a piston cylinder apparatus. An experimental technique has been devised in which the fluid, which should be set free during phengite decomposition at about 950°C and 3.5 GPa, would be triggered by a temperature gradient of about 50 K to infiltrate through a perforated Au-foil the hotter part of the capsule, containing the model mantle material. Crystallization of phlogopitic mica and Al-rich enstatite at the boundary phengite – (forsterite + enstatite), representing the „slab – mantle" contact region, indicates successful experimental simulation of mantle wedge metasomatism. Cs-Rb exchange coefficients K_D, determined from compositions of newly formed phlogopitic micas, recrystallized phengite and of an amorphous phase, representing the quenched liquid, agree well with recently determined alkali-fractionation data between micas and fluid. The composition of the quenched liquid is rich in alkali, aluminium, silicon, and poor in magnesium, which is in agreement with fluid solubility data determined in earlier experimental studies at similar conditions.

Key-words: mantle metasomatism, phlogopite, phengite, experimental study, LILE-fractionation.

Introduction

It is generally accepted that one of the important fluid-induced processes within subduction zones is the metasomatic alteration of the mantle wedge triggered by the breakdown of hydrous phases within the descending lithosphere. This process is strongly associated with, *e.g.*, the principles of dehydration within the subducting slab, the fluid transport through the mantle wedge, magma production at active plate margins, and element cycles leading to typical trace-element and alkali-signatures in subduction-related island-arc basalts.

As the result of infiltration of an alkali-rich slab-derived fluid, phlogopite ($KMg_3[AlSi_3O_{10}](OH)_2$) crystallization has been proposed to occur at the base of a mantle wedge overlying the subducting slab (Sudo & Tatsumi, 1990). In Fig. 1 the thermal structure of the SW Japan subduction zone calculated after Peacock & Wang (1999) is shown, together with the proposed locations of the stabilities of phlogopite and amphibole within the mantle wedge. For the subduction zone of SW Japan, formation of phlogopite can be assumed at the bottom of the mantle wedge exceeding depths of about 100 km and for temperatures lower than about 1200 °C. Towards lower depths amphibole might be the relevant OH-containing phase formed from alkali-metasomatism within the mantle overlying a subducted oceanic slab. Among hydrous phases relevant for subduction zone environments, K-richterite and phlogopite have the highest thermal stabilities (Modreski & Boettcher, 1972), both extending to high pressures above 10.0 GPa (Sudo & Tatsumi, 1990). From phase equilibrium calculations, Wyllie & Sekine (1982) proposed the formation of phlogopite within the mantle as the result of reaction between magma, rising from the subducted crust, and the mantle peridotite. Knowledge how, where, whether, and to which amount phlogopite can be formed within the metasomatized mantle is of importance, because new crystallization of phlogopite within the mantle would play an important role by altering the alkali characteristics of subduction zone related magmas (Tatsumi & Nakamura, 1986). Additionally, this would also explain the occurrence of phlogopite in xenoliths of harzburgites and lherzolites (*e.g.*, Zanetti *et al.*, 1999; Griffin *et al.*, 1999) or even as inclusions within diamonds derived from larger depths (*e.g.*, Zhang *et al.*, 2000).

Important candidates of hydrous minerals for transporting water into the upper mantle during subduction of sediments and basalts are phengitic micas, which compositionally fall along the muscovite ($KAl_2[AlSi_3O_{10}](OH)_2$) – celadonite ($KMgAl[Si_4O_{10}](OH)_2$) solid solution join. Experimental studies on the stability of phengitic muscovite (Schmidt, 1996; Domanik & Holloway, 1996) indicate that phengite persists to depths much greater than the zone of

0935-1221/03/0015-0641 $ 3.15
DOI: 10.1127/0935-1221/2003/0015-0641

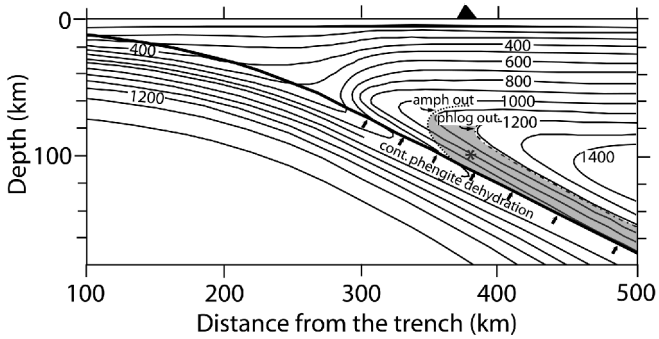

Fig. 1. Thermal structure of the SW Japan subduction zone calculated after Peacock & Wang (1999), together with the proposed locations of stability of phlogopite (Modreski & Boettcher, 1972) and amphibole (Green, 1982) within the mantle wedge. The area phlogopite can be formed metasomatically is shaded. Amphibole out (dotted line), phlogopite out (dotted-dashed line). The asterisk indicates PT-conditions of the experiment. Arrows mark the assumed rise of alkali-rich fluids generated by the continous phengite dehydration within the decending slab.

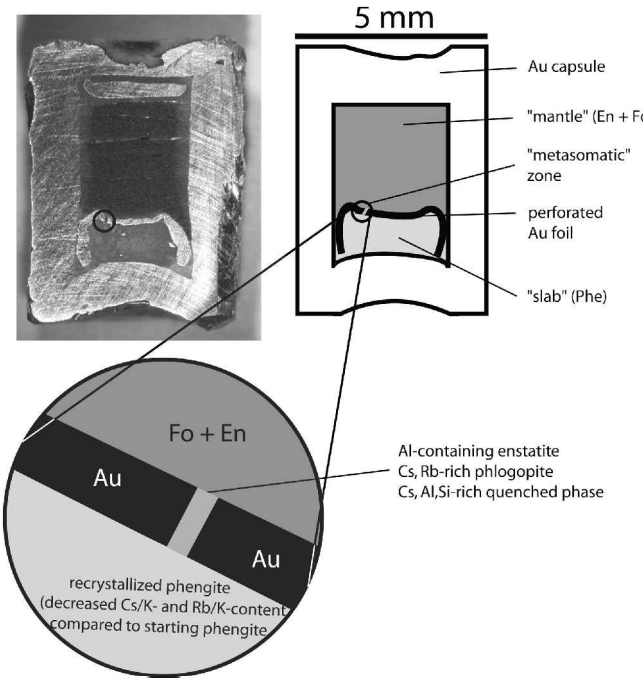

Fig. 2. Schematic drawings and photograph of the cutted Au-capsule after the experiment. The dark part at the top of the capsule represents the recrystallized mantle assemblage consisting of forsterite and enstatite. The light part at the bottom consists of recrystallized phengite and Cs-rich anhedral phase. Additionally, the marked area at the contact (see Fig. 3), representing the „metasomatic zone" is shown in detail. Abbreviations: Phe: phengitic mica; En: enstatite; Fo: forsterite.

melt generation beneath arcs (80 – 150 km). Within a descending slab, phengite should continously decompose to omphacite, enstatite, coesite and a K-rich fluid (Schmidt, 1996). In analogy to phlogopite, Rb and Cs can structurally replace K within phengite completely and both micas are therefore important sources and sinks of large ion lithophile elements (LILE) and hydrous components within subduction zone environments. The cross-arc geochemical variations of alkalis, observed as a function of the depth of the Benioff zone (*e.g.*, Ryan *et al.*, 1995) are believed to be mainly influenced by the fractionation behaviour of Cs, Rb and K between fluid and phengites at different slab depths (Melzer & Wunder, 2000). However, the alkali budget within the mantle wedge would be drastically altered, assuming metasomatic phlogopite crystallization in the mantle as the result of infiltration of slab derived fluid, released from phengite-decomposition within the slab. In such a scenario, the fluid composition would change on its way through a phlogopite-bearing mantle wedge, according to the LILE-partition coefficients of the system phlogopite – fluid (Melzer & Wunder, 2001), which differ from those of the system phengite – fluid (Melzer & Wunder, 2000).

The main goal of this experimental study was to better understand metasomatic processes within the mantle wedge triggered by fluids derived from a subducting slab. Thus, to simulate the metasomatic effects of such an event in the lithospheric mantle, the process of phengite dehydration followed by reactions between the expelled fluid and mantle material was studied at PT-conditions relevant for subduction zones. Another focus was set on the distribution of K, Rb and Cs between solid phases and coexisting fluids in order to test the recently determined LILE-fractionation data between micas and fluids (Melzer & Wunder, 2000, 2001).

Experimental

The experimental assemblage consisting of the simplified model of slab and mantle material is shown in Fig. 2. Within a gold capsule (10 mm length, 1 mm wall thickness, 5 mm outer diameter) about 1/3 of the volume (about 40 mg) was filled with synthetic phengite, placed at the bottom of the capsule. This part should represent the subducted slab material. The upper part of the capsule was filled with a homogeneous mixture of synthetic Fe-free forsterite and clinoenstatite (about 90 mg) of the weight proportion 3:1. This part should represent the overlying mantle wedge. To avoid direct chemical contact, the lower and upper materials were separated by a perforated, about 0.2 mm thick Au-foil.

The experiment was performed in a conventional end-loaded piston-cylinder apparatus at 3.5 GPa for three days. The experimental temperature of 1000 °C was monitored by using a chromel-alumel thermocouple, which was positioned at the top of the capsule. The PT-conditions of the run lie within the stability-field of the assemblage phlogopite + enstatite + vapor after Modreski & Boettcher (1972). A temperature gradient of about 50 K occurs between the bottom and the top of the capsule. The temperature gradient was calculated from a 3D-Finite-Difference scheme recently developed for modeling the temperature distribution in piston-cylinder experiments (Schilling & Wunder, submitted). For the experimental approach chosen it was assumed that the fluid, which should be set free during phengite decomposition at about 950 °C, would be triggered by the temperature gradient to infiltrate the hotter part of the capsule through the perforated Au-foil. No additional water was added. Nevertheless, as the starting materials were not dried before the

Table 1. EMP analyses of starting phengite and product phases (excluding enstatite).

	Phengite (starting mat.) 11 analyses	Phengite (product) 25 analysis	Phlogopite (product) 7 analyses)	Amorphous phase (product) 7 analyses
SiO_2	50.09(4.87)	46.94(1.08)	42.57(0.98)	56.20(11.47)
Al_2O_3	23.48(3.14)	25.82(0.88)	18.04(0.95)	11.47(1.31)
MgO	4.89(1.89)	5.26(0.52)	18.74(2.25)	0.20(0.06)
K_2O	8.10(1.41)	9.06(0.34)	7.17(0.65)	3.73(1.03)
Rb_2O	1.40(0.33)	1.42(0.11)	1.61(0.17)	0.90(0.06)
Cs_2O	1.60(0.63)	1.60(0.28)	2.86(1.14)	5.39(1.82)
Sum	89.56(6.69)	90.09(1.02)	90.97(1.44)	77.89(12.22)
Mica compositions based on 22 oxygens				
Si (IV)	7.11(0.24)	6.71(0.10)	6.22(0.09)	
Al (IV)	0.89(0.12)	1.29(0.05)	1.78(0.12)	
Al (VI)	3.04(0.39)	3.05(0.11)	1.33(0.09)	
Mg (VI)	1.03(0.34)	1.12(0.11)	4.07(0.43)	
K (XII)	1.47(0.30)	1.65(0.07)	1.33(0.11)	
Rb (XII)	0.13(0.03)	0.13(0.01)	0.15(0.02)	
Cs (XII)	0.10(0.04)	0.10(0.01)	0.18(0.07)	

2 σ uncertainties are given in parentheses

experiment, small amounts of water, not exceeding 0.3 wt.% (*e.g.*, Wunder & Schreyer, 1991), might be absorbed at the surface of the fine-grained synthetic silicates.

Synthesis conditions of forsterite (Mg_2SiO_4) and clinoenstatite ($MgSiO_3$) used were already described by Wunder & Schreyer (1997). The grain size of both phases was < 5 µm. Phengite used as starting material was synthesized from oxide mixtures and 2 molal aqueous (K,Rb,Cs)-containing chloride solutions at 2.0 GPa, 600°C. Details of the phengite synthesis technique were described by Melzer & Wunder (2000). As characterized by X-ray powder diffraction, the run product consisted of phengite only. Phengite had grain sizes mostly of < 10 µm in diameter and < 1 µm in thickness. Starting phengitic micas had the composition $(K_{0.74(15)}Rb_{0.06(2)}Cs_{0.05(2)})Al_{1.52(19)}Mg_{0.52(17)}[(Al_{0.45(6)}Si_{3.55(12)})O_{10}/(OH)_2]$ (Table 1).

After the experiment, the capsule was cut vertically and polished samples for scanning electron microscopy (SEM) and electron microprobe (EMP) analyses were prepared. SEM investigations were done with a Zeiss DSM962-microscope. For EMP analyses a Cameca SX100 microprobe using the PAP correction mode (Pouchou & Pichoir, 1984) was used. Counting times for all elements were 20 s on the peak position and 10 s on the background of each side of the peak. Operating conditions were 15 kV and 20 nA. Well defined natural minerals were used as standards (wollastonite: Si; tremolite: Mg; orthoclase: K, Al). For Rb-analyses synthetic Rb-feldspar ($RbAlSi_3O_8$) was used. Cs was standardized on synthetic pollucite ($CsAlSi_2O_6$).

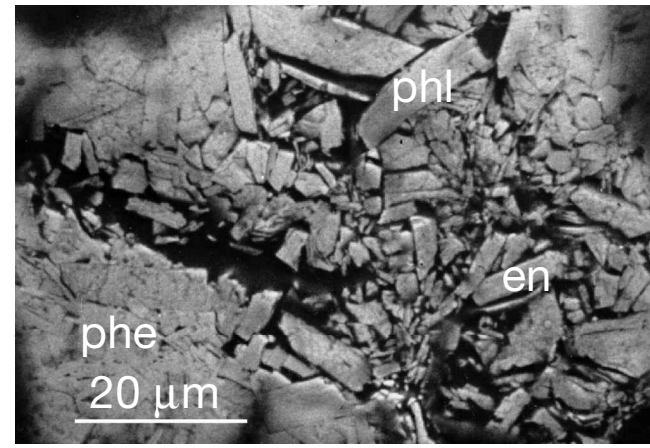

Fig. 3. SEM image showing a magnification of the marked area (see Fig. 2) with newly formed phlogopitic micas, Al-rich enstatite, recrystallized phengite and Cs-rich phase in cavities between mineral grains. The Au-foil is not visible. Abbreviations: phe: phengitic mica; en: enstatite; phl: phlogopitic mica.

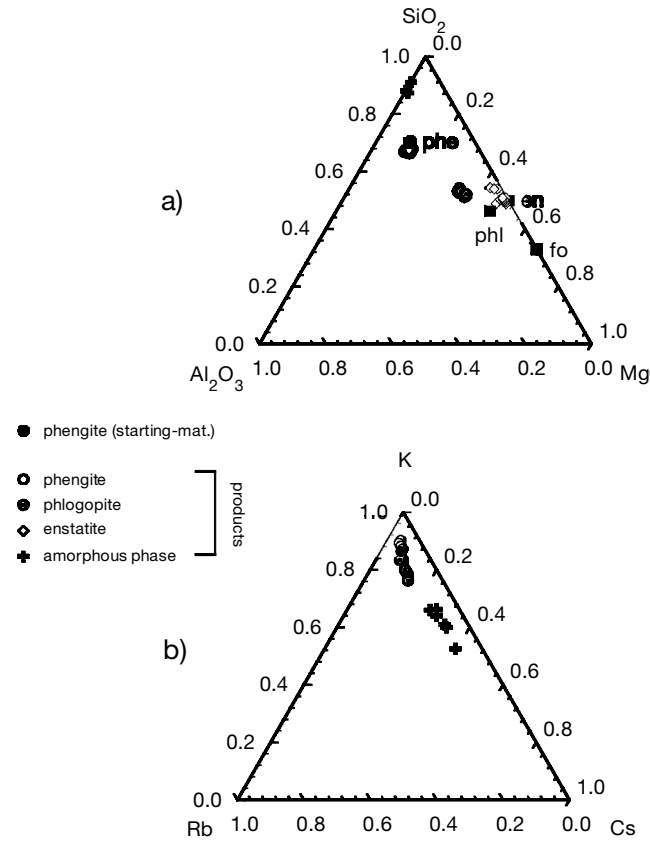

Fig. 4. Compositions of starting materials and product phases (see legend) plotted in the ternary systems a) MgO-Al_2O_3-SiO_2 (molar fractions) and b) Cs-Rb-K (molar ratios). Abbreviations: see Fig. 3.

Results

The first optical impression of the run product using a binocular was that most parts of the starting material had not changed significantly. The lower part still consisted of phengite, the upper part of a mixture of forsterite and enstatite. Newly formed minerals were visible only directly at the contact between the mantle and the slab material (Fig. 3). Using SEM and EMP these were identified as phlogopite and enstatite. Further SEM investigations indicate a complete recrystallization of phengite as well as forsterite and

Table 2. Results of EMP analyses of newly formed enstatite.

distance from contact [μm]	0	2	5	8	23	27	29	32	84	119
SiO_2	60.00	60.53	59.92	58.94	60.13	60.30	59.81	59.47	59.33	60.67
Al_2O_3	1.60	1.23	1.23	1.33	1.19	1.31	1.15	1.20	0.74	0.10
MgO	39.09	38.74	39.13	38.26	39.16	39.10	39.16	38.81	40.01	39.88
Sum	100.69	100.50	100.28	98.53	100.48	100.71	100.12	99.48	100.08	100.65
Structural formulae (calculated for O = 6)										
Si	1.992	2.006	1.993	1.995	1.996	1.996	1.993	1.994	1.982	2.011
Al(tot)	0.082	0.048	0.048	0.053	0.046	0.051	0.045	0.047	0.029	0.004
Al(T)	0.008	0.0	0.007	0.005	0.004	0.004	0.007	0.006	0.018	0.0
Al(M1)	0.074	0.048	0.041	0.048	0.042	0.047	0.038	0.041	0.011	0.004
Mg(tot)	1.898	1.914	1.94	1.93	1.937	1.93	1.945	1.94	1.992	1.971
Mg(M1)	0.926	0.952	0.959	0.952	0.958	0.953	0.962	0.959	0.989	0.996
Mg(M2)	0.972	0.962	0.981	0.978	0.979	0.977	0.983	0.981	1.0	0.975
□ (M2)	0.028	0.038	0.019	0.022	0.021	0.023	0.017	0.019	0.0	0.025

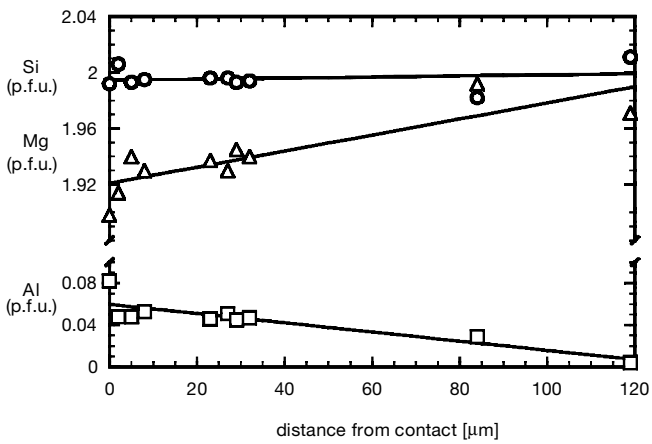

Fig. 5. Change of the chemical composition of Al-containg enstatite in the region of the contact zone (see Fig. 2).

enstatite. Compared to the fine grained starting materials, the run product showed considerably larger grain sizes.

The grain size of the product phengite was commonly > 20 μm (Fig. 3). The compositional variation of the product phengite is rather small, indicating a rather homogeneous composition over the complete lower part of the capsule. Compared to the starting material, the product phengite, the composition of which was determined as $((K_{0.83(4)}Rb_{0.06(1)}Cs_{0.05(1)})Al_{1.53(6)}Mg_{0.56(6)}[(Al_{0.64(3)}Si_{3.36(5)})O_{10}/(OH)_2])$, has higher K/Cs- and K/Rb-ratios and a lower celadonite-component (Table 1, Fig. 4a, b). Notwithstanding the lack of a limiting assemblage, this latter result is in agreement with the known T-dependence of the composition of potassic white micas (*e.g.*, Velde, 1965; Massonne & Schreyer, 1987).

Enstatite in the contact region is up to 10 μm in length (Fig. 3) and contains significant amounts of aluminium (Table 2). Al-containing enstatite was detected over a distance of about 120 μm (Fig. 5) directly above the contact zone. The Al-content of enstatite decreases with increasing distance from the „slab – mantle“ contact (Fig. 5). Enstatite of the highest Al-contents (about 0.08 Al p.f.u., based on 6 oxygens), directly from the contact zone contains about the same Al-amount as determined by Gasparik & Newton (1984) for enstatite synthesized at similar PT-conditions in the system $MgO\text{-}Al_2O_3\text{-}SiO_2$. The enstatite analyses (Table 2) indicate that its composition is influenced by two combined substitution mechanism: the Tschermak substitution (Al + Al = Mg + Si) and a substitution towards a hypothetical termed „Mg-Eskola pyroxene“-component ($\square_{0.5}Mg_{0.5}Al[Si_2O_6]$) after Fockenberg & Schreyer (1997). The alkali content of enstatite is close to the detection limit of the EMP. The same is true for the alkali and Al_2O_3 content of forsterite.

Newly formed phlogopitic micas are up to 30 μm in length and 10 μm in width (Fig. 3). The phlogopitic micas are rather homogeneous in composition (Table 1), $((K_{0.77(6)}Rb_{0.07(1)}Cs_{0.09(3)})Al_{0.67(5)}Mg_{2.03(21)}[Al_{0.89(6)}Si_{3.11(5)}O_{10}/(OH)_2])$. These were only detected within the about 120 μm large Al-enstatite containing contact zone. The phlogopitic micas are rather rich in Al indicating a large eastonite-component ($KMg_{2.5}Al_{0.5}[Si_{2.5}Al_{1.5}O_{10}](OH)_2$). In comparison to product phengite, the newly formed phlogopitic micas are enriched in Cs and Rb.

The analytical total oxid sums of phlogopite and phengite determined by EMP analyses of about 90 wt.% (Table 1) are significantly smaller than the expected values of about 95 wt.%. This might partly be explained due to alkali-loss during EMP measurements. However, Wunder & Melzer (2002) have recently demonstrated that synthetic phlogopites often exhibit incomplete occupation of the interlayer site as the result of a talc component within phlogopite. The EMP analyses given in Table 1 indicate twelve-fold vacancies for both, phlogopite and phengite.

A Cs-, Al-, and Si-rich, almost Mg-free phase was detected by EMP analyses in cavities between phengite grains and within the groundmass of the contact zone. According to the low totals (Table 1) this anhedral, perhaps amorphous phase is probably water-rich and might therefore represent the quenched liquid. It could not be clarified whether the high standard deviation of the EMP analyses (Table 1) is due to

inhomogeneous composition of the phase or due to analytical problems resulting from the small, irregular size of the phase.

Discussion

According to the Rb-, K-, Cs-partitioning between phengite and fluid (Melzer & Wunder, 2000), and phlogopite and fluid (Melzer & Wunder, 2001), a fluid in coexistence with phengite or phlogopite must be relatively enriched in Cs and depleted in Rb at the PT-conditions of the experiment. This agrees well with the composition of the phase observed in pockets between phengite grains and within the contact zone, which is Cs-rich and relatively poor in Rb. Therefore, one might assume that the quenched material represents the liquid phase at elevated temperatures and pressures of the experiment. The alkali-content of recrystallized phengitic muscovites, newly formed phlogopitic micas, and of the Cs-rich phase are shown in Fig. 4b. The observed higher Cs- and Rb-contents within phlogopite compared to phengite are in agreement with the recently determined LILE-partition coefficients of the systems phlogopite – fluid and phengite – fluid. Therefore, this indicates that both solid phases were in contact with the detected Cs-rich liquid. In Table 3 the Cs-Rb exchange coefficiens K_D for the systems phlogopite/liquid and for phengite/liquid as calculated from the analyses given in Table 1 are compared with the solid/fluid-values determined by Melzer & Wunder (2000, 2001) for the same systems at comparable PT-conditions. The good agreement of these values indicate that equilibrium has been reached in our experiment and that the composition of the liquid did not change drastically during the quenching process.

According to Schmidt (1996), phengite continously decomposes to omphacite, enstatite, coesite and a K-rich fluid during the subduction process. As we performed the experiment in a Ca-, Na-, Fe-free system, we propose formation of a Cs-rich liquid during the recrystallization process of phengite, which might be initiated by small amounts of water absorbed at the surface of the starting materials due to the reaction:

starting phengite + water ⇔
product phengite + Cs-rich liquid 1. (1)

Tentatively, we estimate that only a few percent of the starting phengite decomposed during recrystallization. Due to the obviously small amount of liquid available in our experiment, the model assemblage for the mantle wedge only shows symptoms of metasomatism within the 120 µm large range at the contact zone, where phlogopitic micas and Al-containing enstatite were observed. The change of the chemical composition of enstatite with distance to the direct contact zone (Fig. 5) might be seen as evidence of non-equilibrium and reminds to the result of a beginning ion exchange process operating within a chromatographic column. However, for a quantitative mass balance calculation the data base (*e.g.*, the amount of liquid available) is too uncertain.

Table 3. Cs-Rb-exchange coefficients K_D for phlogopite, phengite/fluid as determined by Melzer & Wunder (2000, 2001), and in this study.

	M & W (2000)*	M & W (2001)**	this study
$K_D^{phl\text{-}fluid}$(Cs-Rb)	–	0.20 ± 0.07	0.19
$K_D^{phl\text{-}fluid}$(Cs-Rb)	0.34 ± 0.10	–	0.30

*Melzer & Wunder (2000); K_D determined at 4.0 GPa, 800°C
**Melzer & Wunder (2001); K_D determined at 4.0 GPa, 700°C

The pressure and temperature conditions chosen within our experiment lie within the stability field of enstatite + phlogopite + vapor as determined experimentally by Modreski & Boettcher (1972) in the model system $KAlSiO_4$ – Mg_2SiO_4 – SiO_2 – H_2O. Further they determined that for a pressure of 3.5 GPa and at temperatures above about 1180°C this assemblage incongruently melts to forsterite + liquid. Phlogopitic micas and Al-rich enstatite might therefore be formed by the reaction:

forsterite + Cs-rich liquid 1 ⇔
phlogopitic mica + Al-rich enstatite + Cs-rich liquid 2. (2)

Wyllie & Sekine (1982) proposed that this phlogopite-forming reaction is important for hybridization of the mantle wedge overlying an subducted oceanic crust. According to the experimentally determined LILE-distribution between fluid and phlogopite (Melzer & Wunder, 2001) and fluid and phengite (Melzer & Wunder, 2000), the liquid 2 produced according to reaction (2) should be decreased in Cs relative to the liquid 1 formed from reaction (1). The total alkali-concentration of about 10 wt.% determined for the Cs-rich phase is smaller than the K_2O-solubility of 25 wt.% determined by Ryabchikov & Boettcher (1980) for liquid in equilibrium with phlogopite and forsterite at 3 GPa, 1100°C. This difference might either result from the different assemblages investigated and/or the slightly higher temperatures and lower pressures compared to the PT-conditions of our experiment. Ryabchikov & Boettcher (1980) calculated a dissolved silicate component of about 50 wt.% and a K_2O/Al_2O_3-ratio close to unity for the liquid. Both, the SiO_2-solubility and the alkali(total)/Al_2O_3-ratio determined in this study for the quenched material (Table 1) are in good agreement to the data given by Ryabchikov & Boettcher (1980). The large eastonite-component of the newly formed phlogopitic micas further indicates rather high Al_2O_3-concentrations in the liquid at the PT-conditions of the experiment. Similar high Al_2O_3-solubilities in fluid, as additionally indicated herein from the composition of the Cs-rich phase (Table 1), have recently been observed by Feenstra & Wunder (2002) for experiments on the dehydration of diaspore up to 4.0 GPa, and by Domanik & Holloway (1996) in experiments on the stability of phengite at pressures above 5.0 GPa. Our experiment provides evidence that pyroxene, which is metasomatically formed at the contact zone slab – mantle from an ascending fluid produced by phengite decomposition within the slab must be enriched in aluminium. This might have consequences on the trace element partitioning between pyroxenes and fluid or melt, because it is known from experimental and theoretical studies (*e.g.*, Colson *et al.*, 1988), that partition coefficents are strongly de-

pendent on pressure, temperature and compositions of coexisting solid and liquid phases.

According to Wyllie & Sekine (1982), the location of phlogopitic mantle metasomatism strongly depends on the geometry and thermal structure of the subduction zone. For the rather hot subduction zone of SW Japan shown in Fig. 1, phlogopite crystallization initiated by alkali-rich fluids appears to exceed 100 km in an about 20 km thick seam in the hanging-wall wedge. In this region the temperatures, cooled by the underlying slab, are cold enough, to allow stability of phlogopite and incongruent melting only occurs at higher temperatures. For colder subduction zones than shown in Fig. 1 (*e.g.*, Peacock & Wang, 1999, their Fig. 2a), the stability of amphibole is pulled down within the mantle and phlogopite formation is only possible at larger depths. Additionally, the seam phlogopite can exist within, is decreased in the cold compared to the hot subduction zone, because the position of isotherms within the overlying mantle wedge are more narrow (Peacock & Wang, 1999, their Fig. 2a, b).

It is rather difficult to estimate the amounts of phlogopite formed within a metasomatized mantle wedge from the results of our experiment. However, this study indicates that even small amounts of an alkali-rich agent produced by recrystallization and little phengite dehydration in the experiment led to phlogopite formation. Assuming that phlogopite metasomatism exclusively is produced by continous phengite dehydration within the slab, the depth and amount of phlogopite formation in the mantle would be limited by phengite stability and by the amount of phengite available in the descending slab. According to Schmidt (1996) the maximum depth phengite persists within a cold subduction zone is about 300 km. This value would be reduced within warmer subduction regimes. The modal amount of phengite within a metapelite is about 5 % (Schmidt & Poli, 1998). However, the potassium and water released during the continous decomposition of phengite in the subducted slab is surely only partly incorporated into phlogopite, because (1) at low depths amphibole will be formed instead of phlogopite within the mantle wedge, (2) the potassium solubility in clinopyroxene (Harlow & Veblen, 1991) continously increases with pressure, and (3) perhaps other alkali- and/or water-containing phases (*e.g.*, K-richterite) are formed within the mantle from the ascending fluid in chemically more complex systems and at PT-conditions differing from those performed in this study.

Conclusions

At the PT-conditions of the reactions and for the design used in our experiment, phlogopitic mica and Al-rich enstatite crystallization indicate successful experimental simultion of mantle wedge metasomatism. The Cs-Rb exchange coefficients K_D (Table 3), determined from the compositions of recrystallized phengite, newly formed phlogopite, and of the Cs-rich amorphous phase agree with recently determined fluid – mica LILE-partitioning data, when it is assumed that the Cs-rich phase represents the composition of the quenched liquid. However, our data are too uncertain to allow a mass balance quantification of the processes occurring at the contact zone. At the PT-conditions of the experiment, the alkali, silicon, and aluminium solubilities are in agreement to former experimental studies. Therefore, during the experiment the water-activity was significantly smaller than 1. This observation is important and has to be taken into account, *e.g.*, into calculations of the depth of dehydration reactions within subduction zones and hybridization of the mantle wedge, which are mostly determined for water activities of 1 (*e.g.*, Peacock, 1990). Therefore, the stabilities shown in Fig. 1 are shifted to lower depths for water activities smaller than 1. The occurrence of only symptoms of metasomatism within the contact zone „slab – mantle“ of the experiment might be due to the obviously rather small amounts of liquid available and only partial decomposition of phengite. This might not to be comparable to the assumed much larger amounts of fluid liberated within the subducted slab.

As our study only represents a very simplified snapshot of slab – wedge interactions, future similarily designed experiments on the same topic should be expanded to other pressures, temperatures, temperature gradients, and chemical systems of more complexity to close the gap of the simple chemical model described here and the natural system.

Acknowledgements: We thank E.M. Schemmert for sample preparation and O. Appelt for her technical assistance at the microprobe. We thank W. Heinrich (Potsdam) for constructive comments on an earlier version of the manuscript and T. Fockenberg (Bochum) and an anonymous reader for their thoughtful reviews.

References

Colson, R.O., McKay, G.A., Taylor, L.A. (1988): Temperature and composition dependencies of trace element partitioning: Olivine/melt and low-Ca pyroxene/melt. *Geochim. Cosmochim. Acta*, **52**, 539-553.

Domanik, K.J. & Holloway, J.R. (1996): The stability and composition of phengitic muscovite and associated phases from 5.5 to 11 GPa: Implications for deeply subducted sediments. *Geochim. Cosmochim. Acta*, **60**, 4133-4150.

Feenstra, A. & Wunder, B. (2002): Dehydration of diasporite to corundite in nature and experiment. *Geology*, **30**, 2, 119-122.

Fockenberg, T. & Schreyer, W. (1997): Synthesis and chemistry of unusual excess-Si aluminous enstatite in the system MgO-Al_2O_3-SiO_2 (MAS). *Eur. J. Mineral.*, **9**, 509-518.

Gasparik, T. & Newton, R.C. (1984): The reversed aluminia contents of orthopyroxene in equilibrium with spinel and forsterite in the system MgO-Al_2O_3-SiO_2. *Contrib. Mineral. Petrol.*, **85**, 186-196.

Green, D.H. (1982): Anatexis of mafic crust and high pressure crystallization of andesite. *in* R.S. Thorpe (Ed.), Andesites. Wiley, London, pp. 465-487.

Griffin, W.L., Shee, S.R., Ryan, C.G., Win, T.T., Wyatt, B.A. (1999): Harzburgite to lherzolite and back again: metasomatic processes in ultramafic xenoliths from Wesselton kimberlite, Kimberley, South Africa. *Contrib. Mineral. Petrol.*, **134**, 232-250.

Harlow, G.E. & Veblen, D.R. (1991): Potassium in clinopyroxene inclusions from diamonds. *Science*, **251**, 652-655.

Massonne, H.-J. & Schreyer, W. (1987): Phengite geobarometry based on limiting assemblages with K-feldspar, phlogopite, and quartz. *Contrib. Mineral. Petrol.*, **96**, 212-224.

Melzer, S. & Wunder, B. (2000): Island-arc basalt alkali ratios: Constraints from phengite-fluid partitioning experiments. *Geology*, **28**, 583-586.

–, – (2001): K-Rb-Cs partitioning between phlogopite and fluid: experiments and consequences on the LILE signatures of island arc basalts. *Lithos*, **59**, 69-90.

Modreski, P.J. & Boettcher, A.L. (1972): The stability of phlogopite and enstatite at high pressures: a model for micas in the interior of the earth. *Am. J. Sci.*, **272**, 852-869.

Peacock, S.M. (1990): Fluid processes in subduction zones. *Science*, **248**, 329-337.

Peacock, S.M. & Wang, K. (1999): Seismic consequences of warm versus cool subduction metamorphism: Examples from southwest and northwest Japan. *Science*, **286**, 937-939.

Pouchou, J.L. & Pichoir, F. (1984): Un nouveau modèle de calcul pour la microanalyse quantitative par spectroétrie de rayons. *X. Rech. Aérosp.*, **3**, 167-192.

Ryabchikov, I.D. & Boettcher, A.L. (1980): Experimental evidence at high pressures for potassic metasomatism in the mantle of the earth. *Am. Mineral.*, **65**, 915-919.

Ryan, J.G., Morris, J., Tera, F., Leeman, W.P., Tsvetkov, A. (1995): Cross-arc geochemical variations in the Kurile arc as a function of slab depth. *Science*, **270**, 625-627.

Schmidt, M.W. (1996): Experimental constraints on recycling of potassium from subducted oceanic crust. *Science*, **272**, 1927-1930.

Schmidt, M.W. & Poli, S. (1998): Experimentally based water budgets for dehydrating slabs and consequences for arc magma generation. *Earth Planet. Sci. Lett.*, **163**, 361-379.

Sudo, A. & Tatsumi, Y. (1990): Phlogopite and K-amphibole in the upper mantle: implication for magma genesis in subduction zones. *Geophys. Res. Lett.*, **17**, 1, 29-32.

Tatsumi, Y. & Nakamura, N. (1986): Composition of aqueous fluid from serpentinite in subducted lithosphere. *Geochem. J.*, **20**, 191-196.

Velde, B. (1965): Phengite micas: Synthesis, stability, and natural occurrence. *Am. J. Sci.*, **263**, 886-913.

Wunder, B. & Melzer, S. (2002): Interlayer vacancy characterization of synthetic phlogopitic micas by IR spectroscopy. *Eur. J. Mineral.*, **14**, 1129-1138.

Wunder, B. & Schreyer, W. (1991): Metastability of the 10Å-phase in the system MgO-SiO_2-H_2O (MSH). What about hydrous phases in subduction zones? *J. Petrol.*, **33**, 877-889.

–, – (1997): Antigorite: High-pressure stability in the system MgO-SiO_2-H_2O (MSH). *Lithos*, **41**, 213-227.

Wyllie, P.T. & Sekine, T. (1982): The formation of mantle phlogopite in subduction zone hybridization. *Contrib. Mineral. Petrol.*, **79**, 375-380.

Zanetti, A., Mazzucchelli, M., Rivalenti, G., Vannucci, R. (1999): The Finero phlogopite-peridotite massif: an example of subduction-related metasomatism. *Contrib. Mineral. Petrol.*, **134**, 107-122.

Zhang, H., Menzies, M.A., Zhao, L., Lu, F., Zhou, X. (2000): Multiphase mineral inclusions in diamonds from Fuxian and Mengyin kimberlites, Eastern China. *J. Conf. Abstr.*, **5**(2), 1125.

Received 9 September 2002
Modified version received 9 December 2002
Accepted 27 March 2003